Multipartite *W* states for chains of atoms conveyed through an optical cavity

D. Gonţa[1,*] and S. Fritzsche[2,3,†]

[1]*Max-Planck-Institut für Kernphysik, P. O. Box 103980, D-69029 Heidelberg, Germany*

[2]*Department of Physical Sciences, P. O. Box 3000, FIN-90014 University of Oulu, Finland*

[3]*GSI Helmholtzzentrum für Schwerionenforschung, D-64291 Darmstadt, Germany*

(Received 14 October 2009; published 25 February 2010)

We propose and work out a scheme to generate the entangled *W* states for a chain of *N* four-level atoms which are transported through an optical cavity by means of an optical lattice. This scheme is based on the combined laser-cavity mediated interaction between distant and equally separated atoms and works in a completely deterministic way for qubits encoded by two hyperfine levels of the atoms. Only two parameters, namely the distance between the atoms and the velocity of the chain, determine the effective interaction among the atoms and, therefore, the degree of entanglement that is obtained for the overall chain of *N* qubits. In particular, we work out the parameter regions for which the W_N states are generated most reliably for chains of $N = 2, 3, 4$ and 5 atoms. In addition, we analyze the sensitivity in the formation of entanglement for such chains of qubits due to uncertainties produced by the oscillations of atoms in optical lattices.

DOI: 10.1103/PhysRevA.81.022326 PACS number(s): 03.67.Bg, 42.50.Dv, 42.50.Pq, 03.67.Mn

I. INTRODUCTION

During the past few decades, quantum entanglement has been found essential not only in studying the nonclassical behavior of composite systems but also as important resource for the engineering and processing of quantum information. Nowadays, numerous applications are known that greatly benefit from having entangled quantum states available, such as super-dense coding [1], quantum cryptography [2], or Grover's quantum search algorithm [3], to name just a few. Despite the recent progress in dealing with composite quantum systems, however, the controlled manipulation of these system and their interaction with the environment remains still a great challenge. In addition to various other implementations of composite quantum systems for quantum control and applications in quantum information, excellent control in generating entangled states has been achieved recently with neutral atoms that are coupled to a high-finesse optical cavity [4,5].

In practice, there are two typical ways to encode a single qubit into the level structure of an atom: Apart from (i) selecting two levels separated by an optical transition frequency (*optical* qubit), one may also utilize two hyperfine levels of—typically—the atomic ground state, sometimes referred to as *hyperfine* qubit. In contrast to the optical qubits, the use of hyperfine qubits has the advantage of long coherence times ($\sim$1 s) and, moreover, such qubits are known to be more robust with regard to external perturbations or stray fields. Finally, a number of microwave techniques have been developed during the past few decades that allow initialization, manipulation, and detection of the states of such qubits [6–8].

However, the hyperfine qubit(s) cannot couple directly to a cavity with a resonant mode frequency in the optical domain. Therefore, a four-level configuration needs to be considered, in which the two hyperfine levels are supplemented by two electronically excited levels which are separated by the optical transition frequency and are compatible with the resonant frequency of the cavity. In order to realize an effective manipulation of the hyperfine qubit by means of the optical cavity, its state must be mapped coherently on the electronically excited states and back to the hyperfine levels, once all the desired atom-cavity interactions have been performed. Indeed, such a indirect coupling between the hyperfine qubit and optical cavity opens a route for the generation of entanglement and more complex quantum states between two or more atoms by means of the cavity-mediated interactions.

Despite the recent progress to couple one single atom to the cavity mode, further control of the atomic motion is necessary in order to manipulate the interaction between cavity and a chain of atoms. At the same time, excellent control of the motion of atomic chains is merely possible by using optical lattices (conveyor belts) [9], which have recently been utilized in various setups of cavity QED [10–12]. In Fig. 1 we displayed a schematic view of such optical lattice in which two counterpropagating laser beams with parallel linear polarization produce an interference pattern in the field strength that gives rise to a series of equidistant potential wells, where neutral atoms can be trapped. These wells allow control of the position of atoms with a submicrometer precision over millimeter distances due to their tight confinement along the lattice axis.

The combination of such a lattice with the (optical) cavity QED setup, however, makes it necessary to revise the evolution of the atom-cavity interaction for a chain of atoms that is *conveyed* by such a lattice through the cavity. In particular, one need to analyze how the spacing between the atoms and velocity of the atomic chain (lattice) will affect the formation of entangled states between the hyperfine qubits. By this revised evolution, moreover, the small sample approximation, i.e., when the spacing between the atoms is considered negligible in comparison to the cavity waist, should be abandoned and the position-dependent effects should be taken into account.

*gonta@physi.uni-heidelberg.de

†s.fritzsche@gsi.de

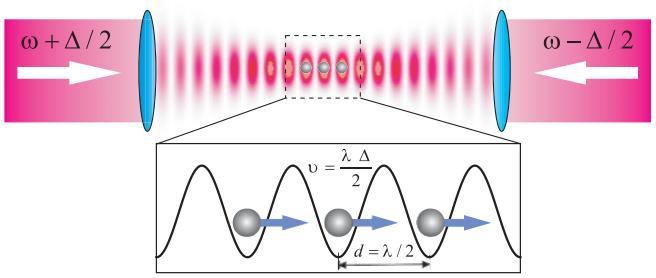

FIG. 1. (Color online) Schematic view of atoms in an optical lattice (conveyor belt). Two focused and counterpropagating laser beams with frequencies $\omega + \Delta/2$ and $\omega - \Delta/2$ give rise to an interference pattern in the field strength with a series of equidistant potential wells in which the atoms can be trapped. The distance d between two neighbored wells is given by (half of) the lattice wavelength λ, while the velocity of the belt υ is determined by the detuning Δ of the two laser beams.

For two hyperfine qubits (in a four-level configuration), we have recently proposed a scheme to generate the maximally entangled state $\frac{1}{\sqrt{2}}(e^{i\phi}|0_1, 1_2\rangle + |1_1, 0_2\rangle)$ by means of the combined laser and cavity mediated interaction [13]. In this reference, we considered the position-dependent coupling between the atoms and cavity which allowed us to describe the formation of entanglement between the two atoms being separated by a macroscopic distance. An effective interaction between the hyperfine qubits was achieved if both the laser and cavity fields are detuned with regard to the atomic transition frequencies (see below). In particular, we demonstrated explicitly how the degree of entanglement depends on the atomic velocities and the spacing between two atoms.

In the present work, we extend this analysis and propose a scheme to generate the entangled W state [14]

$$\frac{1}{\sqrt{N}}(e^{i\phi}\overbrace{|1_1, 0_2, \ldots, 0_N\rangle + \cdots + |0_1, 0_2, \ldots, 1_N\rangle}^{N \text{ terms}}) \qquad (1)$$

between the hyperfine qubits of N (four-level) atoms that are equally distanced from each other and conveyed through the cavity by means of an optical lattice. Similarly to Ref. [13], this scheme works in a completely deterministic way and is based on the position-dependent interaction between distanced atoms which is mediated by the cavity and laser fields. The two parameters that control this atom-cavity-laser interaction are (i) the velocity of the atomic chain along the axis of the lattice and (ii) the distance between the atoms. For the chains consisting of $N = 2, 3, 4$, and 5 atoms, we determine the velocities and distances for which the initially uncorrelated atoms produce the W_N states most reliably. Apart from generation of the W states, we discuss also how the proposed scheme can be implemented most efficiently and analyze how robust are the entangled states with respect to small oscillations in the atomic motion as caused by the thermal motion of atoms in the optical lattice.

The article is organized as follows. In the next section, we first outline our scheme to entangle the hyperfine qubits of N initially uncorrelated atoms. In Sec. III, we then explain and discuss the effective Hamiltonian which describes the atomic evolution; we analyze in particular the parameter (regions) in

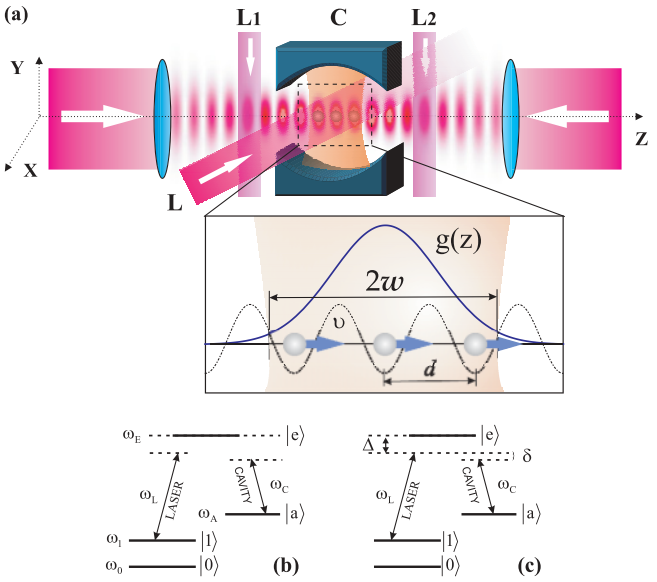

FIG. 2. (Color online) (a) Schematic setup of the experiment. A chain of N neutral atoms passes through a pair of Raman lasers L_1, an optical cavity C with a laser beam L, and a second pair of Raman lasers L_2. The atoms are supposed to move in a chain along the z axis with a constant velocity υ such that the chain crosses the cavity at the antinode. Apart from the cavity waist w, that is just one half of the minimum width of the cavity radiation field, the cavity is also characterized by its position-dependent coupling strength $g(z)$. (b) The atomic four-level Λ-type configuration in the Schrödinger picture and (c) in the interaction picture.

subsections III A– III D for which the states W_2, W_3, W_4, and W_5 are generated most reliably. In Sec. IV, we later discuss a few issues related to the implementation of our scheme and how it is influenced by small oscillations in the motion of the individual atoms, while a short summary and outlook are given in Sec. V.

II. GENERATION OF THE W STATES

We shall first explain the basic idea of the proposed scheme for generating multipartite W entangled states within chains of neutral atoms without going much into details. We assume that the N atoms are initially in a product state and that they are inserted into an optical lattice being equally separated by a distance d as displayed in Fig. 2(a). Moreover, the atoms are supposed to move with a constant velocity υ along the (lattice) z axis such that their position vectors $\vec{r}_i(t) = \{0, 0, z_i^o + \upsilon t\}$ cross the cavity at the antinode and where z_i^o denote the initial position of the ith atom. As briefly outlined above (cf. Fig. 1), this velocity υ and interatomic distance d can be controlled experimentally by adjusting the shift in the frequencies of the two counterpropagating laser beams and by selecting a proper wavelength of the optical lattice, respectively [9].

Each of the N identical atoms represents a (hyperfine) qubit in a Λ-type configuration as displayed in Fig. 2(b), in which the two hyperfine states $|0\rangle$ and $|1\rangle$ are supplemented by the electronically excited states $|e\rangle$ and $|a\rangle$ in such a way that the transitions $|a\rangle \to |1\rangle$ and $|a\rangle \to |0\rangle$ are (electric-dipole)

forbidden due to the angular momentum and parity selection rules. Initially, the atoms are prepared in the product state

$$|1_1, 0_2, \ldots, 0_N\rangle \equiv |1_1\rangle \times |0_2\rangle \times \cdots \times |0_N\rangle, \tag{2}$$

where the numbering corresponds to the (increasing) coordinates $z_1^o, z_2^o, \ldots, z_N^o$ of atoms along the z axis. By this assumption, therefore, the qubits are loaded to the cavity in the *reverse* order, i.e., qubit No. 1 corresponds to the last atom inside the chain.

Just before each atom enters the cavity, its electronic population is transferred from the state $|0\rangle$ to the state $|a\rangle$ with a pair of (slightly) off-resonant laser beams that are coupled to the atomic transitions $|0\rangle \overset{1}{\rightarrow} |e\rangle \overset{2}{\rightarrow} |a\rangle$. This population transfer is known as the two-photon Raman process and can be implemented, for example, by means of two phase-locked laser diodes [6]. Below, we shall briefly refer to this transfer in the population as the Raman pulse and shall distinguish between the Raman zones L_1 and L_2 in front and behind the cavity [see Fig. 2(a)]. In this notation, the Raman pulse L_2 is utilized to perform the population transfer $|a\rangle \overset{2}{\rightarrow} |e\rangle \overset{1}{\rightarrow} |0\rangle$ back to the hyperfine level. Inside the cavity, therefore, the product state (2) becomes $|1_1, a_2, \ldots, a_N\rangle$ since the last atom is unaffected by the Raman pulse L_1.

To explain the mechanism of the cavity-mediated interaction between the atoms in more detail, let us first consider a chain of two atoms prepared in the product state $|e_1, a_2\rangle$ and where each atom is coupled to a detuned optical cavity by the transition $|a\rangle \leftrightarrow |e\rangle$ [cf. Fig. 2(b)]. In this case, both atoms interact due to the cavity-stimulated exchange of a photon: $|e_1, a_2, \bar{0}\rangle \rightarrow |a_1, a_2, \bar{1}\rangle \rightarrow |a_1, e_2, \bar{0}\rangle$ for a initially empty cavity $|\bar{0}\rangle$. This interaction sequence contains in its middle part a virtual state and is independent of the photon number that was initially in the cavity. By following similar lines, therefore, the (initial) atomic state $|e_1, a_2, \ldots, a_N\rangle$ of N atoms in the chain evolves according to the sequence

$$\begin{aligned} |e_1, a_2, \ldots, a_N, \bar{0}\rangle \rightarrow\ & |a_1, e_2, a_3, \ldots, a_N, \bar{0}\rangle \\ \searrow\ & |a_1, a_2, e_3, \ldots, a_N, \bar{0}\rangle \\ & \vdots \\ & |a_1, a_2, a_3, \ldots, e_N, \bar{0}\rangle, \end{aligned} \tag{3}$$

and where the virtual state $|a_1, \ldots, a_N, \bar{1}\rangle$ has been omitted for brevity. As seen from the sequence (3), the atoms in the chain interact due to the cavity stimulated exchange of a single photon between the originally excited atom and one of the $N-1$ other atoms. This photon exchange, moreover, requires a rather large detuning between the transition frequency of the atoms and the resonant frequency of the cavity mode

$$|(\omega_E - \omega_A) - \omega_C| \gg g(\vec{r}_i), \quad i = 1, \ldots, N, \tag{4}$$

namely such that the cavity remains almost unpopulated in the course of interaction [16]. In the expression above, we have introduced the position-dependent atom-cavity coupling

$$g(\vec{r}) = g_o \exp[-z^2/w^2], \tag{5}$$

which is caused by the variation of the transversal cavity field along the atomic trajectories and where g_o denotes the vacuum Rabi frequency and w the cavity mode waist, i.e., one-half of the minimum width of the cavity field [see Fig. 2(a)].

Recall that according to our scheme, however, the atoms are loaded to the cavity in the product state $|1_1, a_2, \ldots, a_N\rangle$ and hence an intermediate excitation $|1\rangle \rightarrow |e\rangle$ is first needed to bring the atoms to interaction by means of the detuned cavity (see above). In order to realize this excitation, the atomic chain is exposed to a detuned laser beam with frequency ω_L that couples—via a position-independent strength Ω to the $|1\rangle \leftrightarrow |e\rangle$ transition as shown in Fig. 2. With the couplings of the atoms to the both laser and cavity fields, the initial atomic state $|1_1, a_2, \ldots, a_N\rangle$ evolves according to the sequence of intermediate atom-cavity states

$$\begin{aligned} |1_1, a_2, \ldots, a_N, \bar{0}\rangle \rightarrow |e_1, a_2, \ldots, a_N, \bar{0}\rangle \rightarrow |a_1, a_2, \ldots, a_N, \bar{1}\rangle \rightarrow\ & |a_1, e_2, a_3 \ldots, a_N, \bar{0}\rangle \rightarrow |a_1, 1_2, a_3, \ldots, a_N, \bar{0}\rangle \\ \searrow\ & |a_1, a_2, e_3, \ldots, a_N, \bar{0}\rangle \rightarrow |a_1, a_2, 1_3, \ldots, a_N, \bar{0}\rangle \\ & \vdots \qquad\qquad\qquad\qquad \vdots \\ & |a_1, a_2, a_3, \ldots, e_N, \bar{0}\rangle \rightarrow |a_1, a_2, a_3, \ldots, 1_N, \bar{0}\rangle \end{aligned} \tag{6}$$

into the one of the final states $|a_1, 1_2, a_3, \ldots, a_N\rangle, \ldots, |a_1, a_2, a_3, \ldots, 1_N\rangle$, which can have the same probability to occur.

In Refs. [13,15] it was shown that the condition

$$|(\omega_E - \omega_1) - \omega_L| \gg \Omega \tag{7}$$

for the detuning between the atomic transition and laser frequencies ensures that the states $|e_1, a_2, \ldots, a_N\rangle$, $|a_1, e_2, \ldots, a_N\rangle, \ldots, |a_1, a_2, \ldots, e_N\rangle$ remain almost unpopulated. For this reason, condition (7) plays the same role as condition (4) for the atom-cavity interaction which makes the state $|a_1, \ldots, a_N, \bar{1}\rangle$ to be only virtually populated. In the following, we shall omit these unpopulated (intermediate) states and express the sequence (6) in the short form

$$\begin{aligned} |1_1, a_2, \ldots, a_N, \bar{0}\rangle \rightarrow\ & |a_1, 1_2, a_3, \ldots, a_N, \bar{0}\rangle \\ \searrow\ & |a_1, a_2, 1_3, \ldots, a_N, \bar{0}\rangle \\ & \vdots \\ & |a_1, a_2, a_3, \ldots, 1_N, \bar{0}\rangle. \end{aligned} \tag{8}$$

With the evolution (8) of the atomic chain due to the laser-cavity mediated interaction, the entangled W state

$$\frac{1}{\sqrt{N}}(e^{i\phi} \overbrace{|1_1, a_2, \ldots, a_N\rangle + \cdots + |a_1, a_2, \ldots, 1_N\rangle}^{N \text{ terms}}) \tag{9}$$

can be, in principle, generated by adjusting properly the atomic velocity υ and the inter-atomic distance d for a given set of fixed cavity and laser parameters. In the last step of our scheme, the electronic population of each atom that leaves the cavity is (coherently) transferred back from the state $|a\rangle$ to the hyperfine state $|0\rangle$ in order to protect the atom against the spontaneous decay. This back transfer is achieved by applying the Raman pulses L_2 behind the cavity and it produces the state (1) from (9), once all the atoms have left the cavity. By utilizing the proposed scheme, therefore, a multipartite W state can be generated starting from the initial product state (2) that is associated with the chain of N atoms which are conveyed through the cavity.

In the next section, we shall analyze in details of how the laser-cavity mediated evolution (8) depends on the velocity υ and the interatomic distance d when the atomic chain is conveyed through the cavity. In order to take into account these two parameters, we shall consider the position-dependent coupling (5), which gives rise to the time-dependent coupling between the ith atom and the cavity

$$g_i(t) = g_o \exp\left[-\left(z_i^o + \upsilon t\right)^2 / w^2\right], \quad i = 1, \ldots, N, \tag{10}$$

where z_i^o and υ denote the initial position of the ith atom and its velocity along the z axis, respectively.

III. EFFECTIVE HAMILTONIAN AND MULTIPARTITE DYNAMICS

While sequence (6) displays the basic concept of how the cavity-laser mediated interaction is achieved between the atoms, we still have to analyze this coupling quantitatively as to understand how to control it in practice. For this purpose, we shall adiabatically eliminate the intermediate states $|a_1, \ldots, a_N, \bar{1}\rangle$ and $|e_1, \ldots, a_N, \bar{0}\rangle, \ldots, |a_1, \ldots, e_N, \bar{0}\rangle$ from the sequence (6). This shall lead to an effective Hamiltonian that describes the time evolution of N atoms which interact with each other according to the simplified sequence (8).

To outline this elimination process, let us first introduce the short-hand notation

$$\begin{aligned} |\mathbf{V}_1\rangle \to |\mathbf{V}_{N+1}\rangle \to |\mathbf{V}_0\rangle \to |\mathbf{V}_{N+2}\rangle \to |\mathbf{V}_2\rangle \\ \searrow |\mathbf{V}_{N+3}\rangle \to |\mathbf{V}_3\rangle \\ \vdots \qquad \vdots \\ |\mathbf{V}_{2N}\rangle \to |\mathbf{V}_N\rangle, \end{aligned} \tag{11}$$

for the composite states of N identical atoms and the cavity, which corresponds one-to-one to the states from sequence (6). With this notation, the W state (9) refers to the states $|\mathbf{V}_1\rangle, \ldots, |\mathbf{V}_N\rangle$, while the cavity-mediated photon exchange is performed between the state $|\mathbf{V}_{N+1}\rangle$ and (one of) the states $|\mathbf{V}_{N+2}\rangle, \ldots, |\mathbf{V}_{2N}\rangle$, respectively.

For N identical atoms, the evolution of the coupled atoms-cavity-laser system is described by the Hamiltonian

$$\begin{aligned} H = \omega_C\, c^\dagger\, c + \sum_{i=1}^{N} (\omega_1 |1\rangle_i\langle 1| + \omega_E |e\rangle_i\langle e| + \omega_A |a\rangle_i\langle a| \\ + [\Omega e^{-i\omega_L t} |e\rangle_i\langle 1| + g_i(t) c |e\rangle_i\langle a| + \text{H.c.}]), \end{aligned} \tag{12}$$

where the first term describes the cavity energy, with c and $c^\dagger$ being the annihilation and creation operators for a cavity photon acting on the Fock states $|\bar{n}\rangle$, and (the summation of) the second term describes the chain of atoms and their interaction with the laser and cavity. In this Hamiltonian, the interaction of the ith atom and the cavity is based on the time-dependent coupling (10). In the summation of the second term, moreover, each term contains the excitation energies ω_1, ω_E, and ω_A which correspond to the atomic states $|1\rangle$, $|e\rangle$, and $|a\rangle$, respectively.

In order to simplify the analysis of the time evolution associated with the Hamiltonian (12), we switch to the interaction picture by using the unitary transformation [13,15]

$$\begin{aligned} U_I = \exp\left(-i(\omega_1 + \omega_L)t \sum_{i=1}^{N} |e\rangle_i\langle e| - i\omega_1 t \sum_{i=1}^{N} |1\rangle_i\langle 1|\right) \\ \times \exp\left(-i\omega_A t \sum_{i=1}^{N} |a\rangle_i\langle a| - i\,[\omega_L - \omega_A + \omega_1]\, t c^+ c\right). \end{aligned}$$

In this picture, the Hamiltonian (12) takes the form

$$\begin{aligned} H_I &= -\delta c^+ c + \sum_{i=1}^{N} H_i \quad \text{with} \\ H_i &= \Delta |e\rangle_i\langle e| + [\Omega |e\rangle_i\langle 1| + g_i(t) c |e\rangle_i\langle a| + \text{H.c.}], \end{aligned} \tag{13}$$

and where $\Delta = (\omega_E - \omega_1) - \omega_L$ and $\delta = (\omega_L - \omega_C) - (\omega_A - \omega_1)$ refer to the two off-resonance shifts (detunings) of the laser and cavity frequencies, respectively, as depicted in Fig. 2(c). The time evolution of the wave function then follows the Schrödinger equation

$$i\frac{d|\Psi\rangle}{dt} = H_I |\Psi\rangle, \tag{14}$$

where we restrict the wave function $|\Psi\rangle$ to the ansatz

$$|\Psi\rangle = \exp\left(i\frac{\Omega^2}{\Delta} t\right) \sum_{i=0}^{2N} C_i(t) |\mathbf{V}_i\rangle, \quad C_i(0) = \delta_{i1}. \tag{15}$$

For this ansatz, the Schrödinger equation (14) gives rise to a closed system of $2N + 1$ equations ($i = 1, \ldots, N$)

$$\begin{aligned} i\dot{C}_0(t) &= \left(\frac{\Omega^2}{\Delta} - \delta\right) C_0(t) + \sum_{j=1}^{N} g_j(t) C_{N+j}(t), \\ i\dot{C}_i(t) &= \frac{\Omega^2}{\Delta} C_i(t) + \Omega C_{N+i}(t), \\ i\dot{C}_{N+i}(t) &= \left(\frac{\Omega^2}{\Delta} + \Delta\right) C_{N+i}(t) + \Omega C_i(t) + g_i(t) C_0(t), \end{aligned} \tag{16}$$

where the dot denotes the time derivative.

As explained above, the $N + 1$ states $|\mathbf{V}_0\rangle$ and $|\mathbf{V}_{N+1}\rangle, \ldots, |\mathbf{V}_{2N}\rangle$ remain (almost) unpopulated if the atom-cavity and atom-laser detuning satisfy the two conditions (4) and (7), respectively. Therefore, in order to separate these states from Eqs. (16), we utilize the adiabatic elimination procedure which assumes an adiabatic behavior of the functions $C_0(t)$ and $C_{N+1}(t), \ldots, C_{2N}(t)$ or, in other words, that their time derivative vanishes to a good approximation. Together with

condition (7) and conditions

$$|\delta| \gg g(t), \quad |\delta\Delta| \gg \Omega^2, \quad |\delta\Delta| \gg g(t)^2, \tag{17}$$

it is justified to eliminate $N+1$ equations from the system (16). Here, we shall omit further details of this derivation for which the reader is referred to the seminal article [16]. The remaining N (effective) equations for the functions $C_i(t)$, take the form

$$i\dot{C}_i(t) = \sum_{\substack{j=1 \\ (j\neq i)}}^{N} \frac{g_i(t)g_j(t)\Omega^2}{\delta\Delta^2} C_j(t). \tag{18}$$

Due to Eqs. (18) for functions $C_i(t)$ and the adiabatic behavior for functions $C_0(t)$ and $C_{N+1}(t), \ldots, C_{2N}(t)$, the evolution of the overall state of the atomic chain is given by the wave function

$$|\Phi\rangle = \sum_{i=1}^{N} C_i(t)|\mathbf{V}_i\rangle = \exp\left(-i\int_{-\infty}^{t} H_{\text{eff}}\, ds\right)|\mathbf{V}_1\rangle, \tag{19}$$

which is associated with the effective Hamiltonian

$$H_{\text{eff}} = \sum_{\substack{i,j=1 \\ (i\neq j)}}^{N} \frac{g_i(t)\, g_j(t)\, \Omega^2}{2\delta\Delta^2}(S_i^+ S_j^- + S_i^- S_j^+), \tag{20}$$

where $S_i^+ = |1\rangle_i\langle a|$ and $S_i^- = |a\rangle_i\langle 1|$ denote the atomic two-photon excitation and de-excitation operators. Obviously, this Hamiltonian (20) is much simpler and describes the effective atomic evolution (8) as mediated by the combined laser and cavity fields in Eqs. (18). In order to summarize the steps before, we have therefore found that the evolution of four-level atoms is reduced to the evolution of effectively two-level atoms which interact via a two-photon exchange in such a manner that the excited state $|e\rangle$ remains (almost) unpopulated.

When all the N atoms have left the cavity, the wave function (19) becomes in the limit $t \to +\infty$

$$|\Phi\rangle = \exp(-i\mathrm{M})|\mathbf{V}_1\rangle, \quad \mathrm{M} \equiv \int_{-\infty}^{+\infty} H_{\text{eff}}\, ds, \tag{21}$$

where the matrix elements $\mathrm{M}_{ij} = \langle\mathbf{V}_i|\mathrm{M}|\mathbf{V}_j\rangle$ are given by

$$\mathrm{M}_{ii} = 0 \quad \text{and} \quad \mathrm{M}_{ij} = \theta(\upsilon, |i-j|d) \quad \text{for} \quad i \neq j, \tag{22}$$

with

$$\theta(\upsilon, d) = \sqrt{\frac{\pi}{2}}\frac{\Omega^2 g_o^2 w}{\delta\Delta^2\upsilon}\exp\left(-\frac{d^2}{2w^2}\right). \tag{23}$$

The latter expression (23) can be interpreted as the asymptotic coupling for a pair of atoms that move with the same velocity υ and are separated by the distance d from each other. The atomic evolution of the state (21), therefore, is completely characterized by the asymptotic coupling (23) which depends on the two parameters (υ, d) once the frequency shifts and coupling constants δ, Δ, w, g_o, and Ω are fixed by a particular experimental setup.

Let us recall here that, after the atoms have left the cavity, their population in the (electronic) state $|a\rangle$ is transferred coherently back into the hyperfine state $|0\rangle$ by applying the Raman pulses L_2. With this transfer, the wave function (21) then gives the entangled W-class state of N hyperfine qubits

$$|\Phi'_N\rangle = \sum_{i=1}^{N} C_i(\upsilon, d)|\mathbf{V}'_i\rangle, \quad \text{with}$$
$$|\mathbf{V}'_1\rangle = |1_1, \ldots, 0_N\rangle, \ \ldots, \ |\mathbf{V}'_N\rangle = |0_1, \ldots, 1_N\rangle, \tag{24}$$

and where the functions

$$C_i(+\infty) \equiv C_i(\upsilon, d) = \langle\mathbf{V}'_i|\exp(-i\mathrm{M})|\mathbf{V}'_1\rangle \tag{25}$$

are obtained from the exponentiation of the Hermitian operator $(-i\mathrm{M})$. These functions can be computed routinely for any number of atoms N, for instance, by diagonalization of the matrix (22).

The wave function (24), however, has not yet the desired form of a W state (1). In the next subsections, we shall therefore discuss the properties of the W_N states for different values of N and display those υ and d parameters for which the function $|\Phi'_N\rangle$ is equivalent (or close) to the desired W states.

A. Two-partite entangled state

For a chain of just two atoms $(N = 2)$, the wave function (24) takes the simple form [13]

$$|\Phi'_2\rangle = \cos\theta(\upsilon, d)|\mathbf{V}'_1\rangle - i\sin\theta(\upsilon, d)|\mathbf{V}'_2\rangle. \tag{26}$$

From this expression, we readily recognize that the two-partite W_2 states

$$|W_2^{\pm}\rangle = \frac{1}{\sqrt{2}}(e^{\pm i\frac{\pi}{2}}|1_1, 0_2\rangle + |0_1, 1_2\rangle) \tag{27}$$

are obtained (up to a global phase factor) if the condition $\theta(\upsilon, d) = (2n+1)\pi/4$ is satisfied for some integer n. For a fixed set of experimental parameters δ, Δ, w, g_o, and Ω, therefore, a maximum entanglement is obtained only along the solid lines displayed in Fig. 3(a) for $n = 0, 1, 2, 3$. Obviously, the change between maximally entangled (solid lines) and completely disentangled states (dashed lines) happens more and more rapidly as the velocity of the chain is decreased from a certain maximum value (namely for $n = 0$) onward.

Apart from understanding the dynamical parameters (υ, d) for which a maximum entanglement is achieved, it is important also to know how sensitive these states are with regard to small uncertainties in the velocity and interatomic distance. To analyze this sensitivity, Fig. 3(b) displays the *von Neumann entropy* [17]

$$\begin{aligned} E(\upsilon, d) &= -\mathrm{Tr}(\rho\log_2\rho) \\ &= -\cos^2\theta(\upsilon, d)\log_2[\cos^2\theta(\upsilon, d)] \\ &\quad -\sin^2\theta(\upsilon, d)\log_2[\sin^2\theta(\upsilon, d)] \end{aligned} \tag{28}$$

for velocities and distances satisfying $\theta(\upsilon, d) < 2\pi$ and where $\rho = \mathrm{Tr}_2(|\Phi'_2\rangle\langle\Phi'_2|)$ denotes the reduced density operator with regard to the second hyperfine qubit. As expected, the maximal values of the von Neumann entropy, i.e., $E(\upsilon, d) = 1$, are obtained along the lines which are displayed in Fig. 3(a). Moreover, the least rapid variation in the maxima occurs along the $n = 0$ line and for rather small interatomic distances. For small velocities or some larger distance of the atoms, in contrast, a good control of the entanglements of the $|\Phi'_2\rangle$ states becomes more and more difficult.

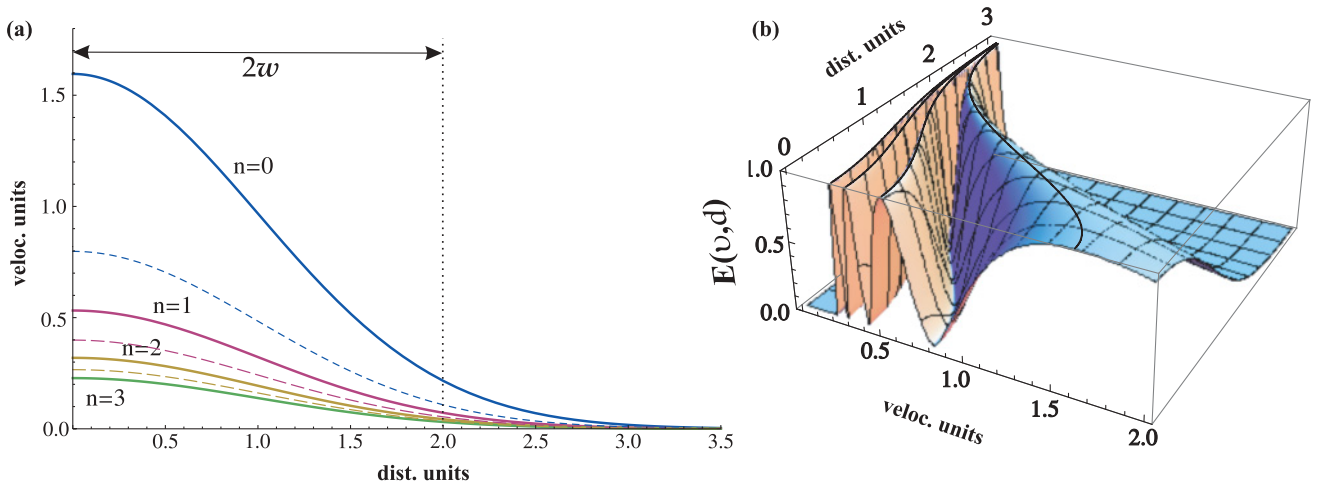

FIG. 3. (Color online) (a) Atomic velocities υ and interatomic distances d for which the initial product state of two atoms $|1_1, 0_2\rangle$ becomes maximally entangled (solid lines). The dashed lines, in contrast, indicate the (υ, d) pairs for which the atomic qubits remain disentangled. (b) Plot of the von Neumann entropy $E(\upsilon, d)$ as a function of the atomic velocity and distance. In all these figures, the velocities υ are displayed in units of $\Omega^2 g_o^2 w/\delta\Delta^2$ and the distances d in units of w.

Figure 3(a) shows that an entanglement between the atoms occurs even for interatomic distances which are larger than $2w$, i.e., twice the cavity waist. In a high finesse cavity, indeed, the Gaussian profile (5) approximates quite well the intracavity field and, thus, it is possible to generate an entangled state even for the atomic separation $d > 2w$. In practice, however, the cavity relaxation and the spontaneous decay of the atoms introduce certain limitations on the distance between the atoms, beyond which it is not possible to generate the entangled state (27). In order to estimate this limitation, we consider the condition [18]

$$N g_o^2 \exp[-2z^2/w^2]/(\kappa\gamma) > 1 \tag{29}$$

which ensures that N atoms couple strongly to the cavity field and, therefore, implies the validity of the effective evolution (20). Here, κ and γ denote the cavity loss rate and the atomic decay rate, respectively. For $N = 2$, the above condition bounds the atomic coordinate to the interval $z_- < z < z_+$ with

$$z_\pm = \pm w\sqrt{\frac{\ln\left[2g_o^2/(\kappa\gamma)\right]}{2}}. \tag{30}$$

Due to these boundaries, therefore, the distance d between two atoms must satisfy

$$\frac{d}{w} < \sqrt{2\ln\left[2g_o^2/(\kappa\gamma)\right]} = \frac{z_+}{w} - \frac{z_-}{w}. \tag{31}$$

For the typical atom-cavity parameters [12]: $\{g_o, \kappa, \gamma\} = 2\pi \times \{10, 0.4, 2.6\}$ MHz, this codition implies the limitation $d < 3.243\ w$. We note that this estimation agrees well with the solid lines from Fig. 3(a) since, for $d > 3.2\ w$, the atomic velocity becomes so small that it would prevent any experimental implementation of our scheme.

B. Tree-partite *W* state

For a chain of three atoms ($N = 3$), the wave function (24) takes the form

$$|\Phi_3'\rangle = \sum_{i=1}^{3} C_i(\upsilon, d)|\mathbf{V}_i'\rangle, \tag{32}$$

with

$$\begin{aligned} C_1(\upsilon, d) &= \frac{-\xi^3\lambda_- + \sqrt{8+\xi^6}(\lambda_+ + 2e^{i\kappa})}{4\sqrt{8+\xi^6}} e^{-i\zeta}, \\ C_2(\upsilon, d) &= -\frac{\lambda_-}{\sqrt{8+\xi^6}} e^{-i\zeta}, \\ C_3(\upsilon, d) &= \frac{-\xi^3\lambda_- + \sqrt{8+\xi^6}(\lambda_+ - 2e^{i\kappa})}{4\sqrt{8+\xi^6}} e^{-i\zeta}, \end{aligned} \tag{33}$$

and where we used the notation $\xi = \exp[-d^2/(2w^2)]$ and

$$\begin{aligned} \lambda_\pm &= \exp[i2\xi\chi\sqrt{8+\xi^6}] \pm 1, \\ \chi &= \sqrt{\frac{\pi}{8}}\frac{\Omega^2 g_o^2 w}{\delta\Delta^2\upsilon}, \\ \kappa &= \xi\chi(3\xi^3 + \sqrt{8+\xi^6}), \\ \zeta &= \xi\chi(\xi^3 + \sqrt{8+\xi^6}). \end{aligned}$$

In order to obtain the state W_3 from wave function $|\Phi_3'\rangle$, we have to determine those pairs (υ, d) for which the equations

$$|C_1(\upsilon, d)| = |C_2(\upsilon, d)| = |C_3(\upsilon, d)| = \frac{1}{\sqrt{3}} \tag{34}$$

are fulfilled. In Fig. 4(a), we displayed the corresponding lines for which the moduli $|C_1(\upsilon, d)|$ (solid), $|C_2(\upsilon, d)|$ (dashed), and $|C_3(\upsilon, d)|$ (dotted) are equal to $1/\sqrt{3}$. The requested W_3 states are obtained for those (υ, d) pairs for which all three types of lines intersect with each other.

As seen from Fig. 4(a), however, the lines for the (moduli of the) functions $C_i(\upsilon, d)$ intersect only if the interatomic distance vanishes. In order to determine the corresponding

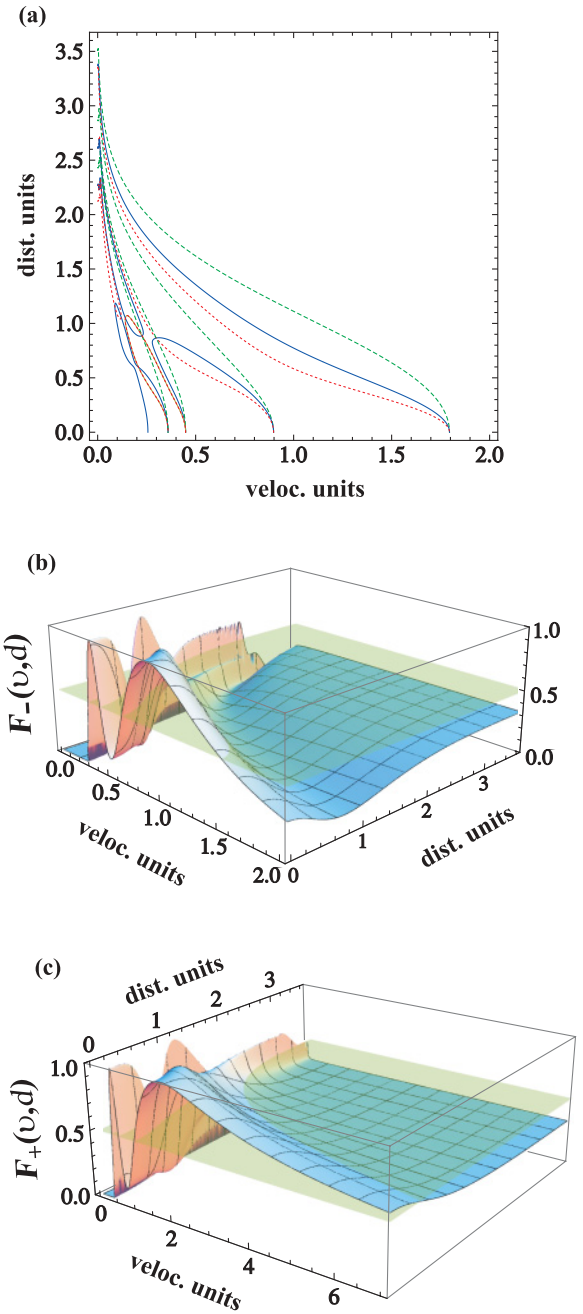

FIG. 4. (Color online) (a) Lines along which the moduli $|C_1(\upsilon, d)|$ (solid), $|C_2(\upsilon, d)|$ (dashed), and $|C_3(\upsilon, d)|$ (dotted) are equal to $1/\sqrt{3}$. These lines correspond to velocities (36) with $n = 0, 1$ and $m = 1, 2$ (in the limit $d \to 0$). (b) Two maxima in the fidelity $F_-(\upsilon, d)$ obtained for velocities (36) with $n = 0, 1$ and $m = 1, 2$ (in the limit $d \to 0$). For guidance of the eyes, the semitransparent layer displays a constant value $F_-(\upsilon, d) = 0.5$. (c) The same as in figure (b) but for the fidelity $F_+(\upsilon, d)$. Again, all velocities υ are displayed in units of $\Omega^2 g_o^2 w/\delta\Delta^2$ and the distances d in units of w.

velocities, we first observe that for $d \to 0$ ($\xi \to 1$), the wave function (32) becomes

$$e^{-i4\chi}\frac{1+2e^{i6\chi}}{3}|\mathbf{V}_1'\rangle + e^{-i4\chi}\frac{1-e^{i6\chi}}{3}(|\mathbf{V}_2'\rangle + |\mathbf{V}_3'\rangle).$$

This expression can be readily cast into the W_3 form

$$|W_3^{\pm}\rangle = \frac{1}{\sqrt{3}}(e^{\pm i\frac{2\pi}{3}}|\mathbf{V}_1'\rangle + |\mathbf{V}_2'\rangle + |\mathbf{V}_3'\rangle) \tag{35}$$

if $\chi = (3n + m)\pi/9$ or, equivalently, if the velocity takes the values

$$\upsilon = \sqrt{\frac{\pi}{8}}\frac{\Omega^2 g_o^2 w}{\delta\Delta^2}\frac{9}{\pi(3n+m)}, \tag{36}$$

with $m = 1, 2$ and n being an integer. To summarize, the vanishing interatomic distance along with velocities (36) are both necessary to obtain the W_3 states due to wave function (32). According to our scheme, however, the atoms are separated by a macroscopic distance which is non-negligible with regard to the cavity waist. Therefore, we may determine the parameter region (υ, d) with the nonzero interatomic distance, for which the two fidelities [17]

$$\begin{aligned} F_{\pm}(\upsilon, d) &= |\langle W_3^{\pm}|\Phi_3'\rangle|^2 \\ &= \tfrac{1}{3}|e^{\mp i\frac{2\pi}{3}}C_1(\upsilon, d) + C_2(\upsilon, d) + C_3(\upsilon, d)|^2, \end{aligned} \tag{37}$$

between the states $|W_3^{\pm}\rangle$ and $|\Phi_3'\rangle$ are larger than the threshold value of $1/2$. These fidelities $F_-(\upsilon, d)$ and $F_+(\upsilon, d)$ are displayed in Figs. 4(b) and 4(c), together with a semitransparent plane in order to delimit the regions for which $F_{\pm}(\upsilon, d) \geqslant 0.5$. While the maximum values $F_{\pm}(\upsilon, d) = 1$ are obtained only for a few velocities and vanishing interatomic distance, there are still (υ, d) regions (with nonzero distance) for which the fidelities become reasonably close to the maximal value. Note, moreover, that the region with $F_+(\upsilon, d) \geqslant 0.5$ is notably larger than those with $F_-(\upsilon, d) \geqslant 0.5$. We conclude, therefore, that from the experimental perspective it might be preferable to generate the $|W_3^+\rangle$ state between three hyperfine qubits by means of the suggested scheme.

C. Four-partite *W* state

For a chain of four atoms ($N = 4$), the wave function (24) can be written as

$$|\Phi_4'\rangle = \sum_{i=1}^{4} C_i(\upsilon, d)|\mathbf{V}_i'\rangle. \tag{38}$$

In contrast to $N = 2$ or $N = 3$, however, the expressions for $C_i(\upsilon, d)$ become rather bulky now and are not displayed here. Recall from the previous subsection that the wave function $|\Phi_3'\rangle$ produced the $|W_3^{\pm}\rangle$ states only for vanishing distances and velocities (36). In this subsection, therefore, we proceed in a similar fashion and consider the wave function (38) with the vanishing interatomic distance ($d \to 0$)

$$e^{-i4\chi}\frac{1+3e^{i8\chi}}{4}|\mathbf{V}_1'\rangle + e^{-i4\chi}\frac{1-e^{i8\chi}}{4}\sum_{i=2}^{4}|\mathbf{V}_i'\rangle.$$

From this expression, the state

$$|W_4\rangle = \tfrac{1}{2}(e^{i\pi}|\mathbf{V}_1'\rangle + |\mathbf{V}_2'\rangle + |\mathbf{V}_3'\rangle + |\mathbf{V}_4'\rangle) \tag{39}$$

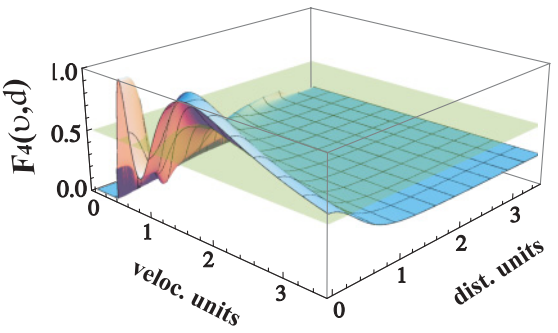

FIG. 5. (Color online) Fidelity $F_4(\upsilon, d)$ for the generation of the W_4 state as a function of the velocity and the interatomic distance. Again, the maximum value $F_4(\upsilon, d) = 1$ is obtained only for vanishing distance ($d = 0$) and velocities (40) with $n = 0, 1$. The semitransparent plane with $F_4(\upsilon, d) = 0.5$ is plotted to guide the eyes; the units are the same as in Figs. 3 and 4.

is readily produced if $\chi = \pi(2n + 1)/8$ or, equivalently, if the velocity takes the values

$$\upsilon = \sqrt{\frac{\pi}{8}} \frac{\Omega^2 g_o^2 w}{\delta\Delta^2} \frac{8}{\pi(2n+1)}. \tag{40}$$

More generally, Fig. 5 displays the fidelity $F_4(\upsilon, d) = |\langle W_4|\Phi'_4\rangle|^2$ for the generation of the W_4 states as a function of the velocity and the interatomic distance due to the wave function (38). Analogous to the last subsection, the maximum fidelity $F_4(\upsilon, d) = 1$ is obtained only for zero distance ($d = 0$) and velocities that fulfill the condition (40). For nonzero distances, nevertheless, there is one broad parameters region for which the W_4 state (39) can be generated with a reasonable high fidelity.

D. $N \geqslant 5$ partite W state

For any other number $N \geqslant 5$ of atoms in the chain, the functions $C_1(\upsilon, d), \ldots, C_N(\upsilon, d)$ can still be computed from the formula (25), and the wave function $|\Phi'_N\rangle$ can be further analyzed with regard to the (υ, d) region, for which the corresponding W_N state is produced most reliably. In order to generate such a state, according to the definition (1), the conditions

$$|C_1(\upsilon, d)| = \cdots = |C_N(\upsilon, d)| = \frac{1}{\sqrt{N}} \tag{41}$$

need to be fulfilled. By performing numerical analysis, however, it turns out that the Eqs. (41) cannot be fulfilled for any choice of the velocity and interatomic distance and, therefore, the fidelity $|\langle W_N|\Phi'_N\rangle|^2$ is always smaller than unity.

Nevertheless, we can display this fidelity as a function of υ and d and determine the region where it takes the highest value. In order to proceed so, however, we still need to specify the *reference* state $|W_N\rangle$, which we are looking in the form

$$|W_N\rangle = \frac{1}{\sqrt{N}} \left(e^{i\phi}|\mathbf{V}'_1\rangle + \sum_{i=2}^{N} |\mathbf{V}'_i\rangle \right) \tag{42}$$

with an unknown phase ϕ. The form of this state has been chosen in line with the previously obtained W states (27), (35), and (39). In order to calculate the unknown phase ϕ in (42), let us first consider the W-class state

$$|\widetilde{\Phi}'_N\rangle = e^{i4\chi} \sum_{k=1}^{N} C_k(\upsilon, 0)|\mathbf{V}'_k\rangle$$
$$= \sum_{k=1}^{N} \frac{1 + (\delta_{k1}N - 1)\exp(i2N\chi)}{N} |\mathbf{V}'_k\rangle, \tag{43}$$

where the velocity υ is such that it makes the expressions

$$\left| |C_1(\upsilon, 0)| - \frac{1}{\sqrt{N}} \right|, \ldots, \left| |C_N(\upsilon, 0)| - \frac{1}{\sqrt{N}} \right| \tag{44}$$

minimal. It can be straightforwardly shown that all the expressions (44) are minimized for the values $\chi = \pi(2n + 1)/(2N)$ or, equivalently, for velocities

$$\upsilon = \sqrt{\frac{\pi}{8}} \frac{\Omega^2 g_o^2 w}{\delta\Delta^2} \frac{2N}{\pi(2n+1)}. \tag{45}$$

Substituting this value for χ, the state (43) then becomes

$$|\widetilde{\Phi}'_N\rangle = \frac{2 - N}{N}|\mathbf{V}'_1\rangle + \frac{2}{N}\sum_{i=2}^{N}|\mathbf{V}'_i\rangle. \tag{46}$$

For a vanishing interatomic distance, therefore, the state $|\widetilde{\Phi}'_N\rangle$ with velocities (45) gives the best approximation to the W_N state.

As we explained in the beginning of this subsection, there are no such (υ, d) pairs for which the Eqs. (41) can be fulfilled. However, we found the state (46) which gives the best approximation to the W_N state (42). By comparing the states $|W_N\rangle$ with $|\widetilde{\Phi}'_N\rangle$ for $N = 4$, we find that the phase ϕ is equal to π and, therefore, the reference state becomes

$$|W_N\rangle = \frac{1}{\sqrt{N}} \left(e^{i\pi}|\mathbf{V}'_1\rangle + \sum_{i=2}^{N} |\mathbf{V}'_i\rangle \right), \quad N \geqslant 4. \tag{47}$$

In order to understand how well the state (46) approximates the above state (47), in Fig. 6(a) we displayed the fidelity $F(N) = |\langle W_N|\widetilde{\Phi}'_N\rangle|^2$. As seen from this figure, the fidelity has its maximum value $F(N) = 1$ for $N = 4$ and decreases monotonically as the number of atoms is increases in the chain. The fidelity drops below the threshold $F(N) = 1/2$ for $N > 15$. We therefore conclude that the state (46) approximates reasonably well the reference state for at least $4 < N < 15$.

Having specified the reference state (47), we can evaluate the fidelities

$$F_N(\upsilon, d) = |\langle W_N|\Phi'_N\rangle|^2; \quad 5 \leqslant N < 15 \tag{48}$$

as functions of the velocity and the interatomic distance. In Fig. 6(b), for instance, we display the fidelity (48) for $N = 5$. According to this figure, moreover, the fidelity reaches its maxima $F_5(\upsilon, d) = F(5) \approx 0.97$ for $d = 0$ and velocities that satisfy the condition (45) with $n = 0, 1$. Let us note here that the typical spacing between two neighbored potentials wells (sites) of an optical lattice is in the submicrometer range [10–12]. As seen from Fig. 6(b), this typical spacing is comparable to the interatomic distance for which the fidelity $F_5(\upsilon, d) \approx 0.9$ is reasonable high and where the typical cavity waist ($w = 20\ \mu$m) has been considered as the distance units. The recent developments in cavity QED, therefore, make it

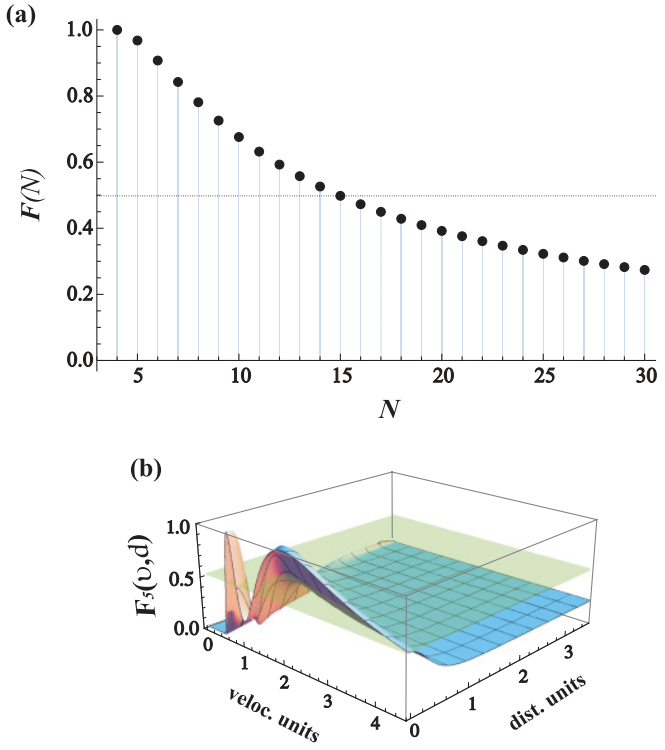

FIG. 6. (Color online) (a) The fidelity $F(N) = |\langle W_N|\widetilde{\Phi}'_N\rangle|^2$ has its maximum value $F(N) = 1$ for $N = 4$ and decreases monotonically as the number of atoms increases. For $N > 15$, it falls below the threshold $F(N) = 1/2$ (dotted line). (b) Fidelity $F_5(\upsilon, d)$ for the production of the $|W_5\rangle$ state due to $|\Phi'_5\rangle$ as a function of the velocity and the interatomic distance. Similarly as in Fig. 5, it reaches its maxima for $d = 0$ and velocities (45) with $n = 0, 1$. The units are the same as in Figs. 3 and 4.

possible to generate the W_5 state by means of the proposed scheme. If we compare, however, the (υ, d) regions for which the fidelities $F_{\pm}(\upsilon, d)$ [Fig. 4(b)–4(c)], $F_4(\upsilon, d)$ [Fig. 5], and $F_5(\upsilon, d)$ [Fig. 6(b)] are higher than the threshold value of $1/2$, we also conclude that these regions become smaller as the number of atoms (in the chain) increases.

IV. REMARKS ON THE IMPLEMENTATION OF THE PROPOSED SCHEME

In our discussions so far, we have always assumed that the velocity and the distance of the atoms in the chain, i.e., their position within the optical lattice, can be controlled exactly. With this assumption in mind, the atom-cavity coupling was described by expression (10). This assumption, however, neglects the transversal components of the cavity field as well as the oscillations of the atoms within the potential well due to their finite temperatures, which include both the axial (along the z axis) and radial (along the x and y axes) oscillations [see Fig. 2(a)]. This additional motion gives rise to a dispersion of the atomic positions and velocities and, thus, leads to uncertainties in selecting the dynamical parameters in our model.

Obviously, any significant uncertainty in the parameters $\{\upsilon, d, \delta, \Delta, g_o, \Omega\}$ will influence the generation of the desired W entangled states. According to our scheme, however, these entangled states are produced when all the atoms have left the cavity. Instead of understanding these parameters as *exact*, therefore, they should refer to the mean values and we need to analyze how small (but realistic) variations in these parameters affect the final state of the atomic chain. For instance, the radial oscillations of the atoms lead to the mean value of the vacuum Rabi frequency $\overline{g}_o$ and axial oscillations to the mean values of the interatomic distance $\overline{d}$ and velocity $\overline{v}$, respectively. Axial oscillations affects also the initial position z_i^o and velocity υ_i of each atom inside the lattice and result in uncertainties $\Delta d_i = \overline{d} - |z_{i+1}^o - z_i^o|$ and $\Delta\upsilon_i = \overline{\upsilon} - \upsilon_i$, where $i = 1, \ldots, N$. Therefore, the plots $E(\upsilon, d)$, $F_{\pm}(\upsilon, d)$, $F_4(\upsilon, d)$, and $F_5(\upsilon, d)$ from Figs. 3–6 should be recalculated as function of the mean values $\overline{\upsilon}$ and $\overline{d}$ and their corresponding uncertainties, respectively.

In order to determine realistic uncertainties for the distance and velocity of the atoms in the chain, we first mention that recent cavity QED experiments allow to position the atoms relative to the cavity antinode with a precision of $\sim 0.1\ \mu$m by utilizing an additional dipole trap acting along the cavity y axis [10]. When compared to the typical cavity wavelength ($\sim 0.8\ \mu$m), such positioning precision leads to the spatial dispersion which, in turn, yields the mean value $\overline{g}_o \approx 0.75 g_o$ that is still good enough for our purposes [see Eq. (17)]. Moreover, the same spatial dispersion implies upper bounds for the uncertainties $|\Delta d/\overline{d}| \lesssim 0.2$ and $|\Delta\upsilon/\overline{\upsilon}| \lesssim 0.1$, if compared with the typical spacing ($\sim 0.5\ \mu$m) between two neighbored potential wells of an optical lattice and the typical atomic velocities (~ 0.5 m/s) along the lattice axis.

For a further analysis of how reliably a given (experimental) setup will generate a particular W state, in Fig. 7 we display the (mean) functions $\overline{E}(\upsilon, d)$, $\overline{F}_{\pm}(\upsilon, d)$, and $\overline{F}_4(\upsilon, d)$ by calculating their average for a certain spread of parameters. For each subfigure 7(a)–7(d), we have randomly chosen 20 uncertainties Δd and $\Delta\upsilon$ from the intervals $[0, 0.2\overline{d}]$ and $[0, 0.1\overline{\upsilon}]$, respectively. By comparing the Figs. 3(c) and 7(a) it can be seen that the von Neumann entropy, for instance, is reduced considerably for its sharp maxima ($n = 3$) and that it remains almost the same around the broad maxima ($n = 0$). Similarly, the mean fidelities which are displayed in Figs. 7(b)–7(d), are considerably reduced for their sharp maxima. These (υ, d) regions for the velocity and interatomic distance in the atomic chain are, therefore, less useful for any practical implementation and only the (υ, d) regions which correspond to the broad maxima of the von Neumann entropy and fidelities are relevant for the generation of entangled W states by means of the proposed scheme.

Finally, we assumed in our treatment that the (center-of-mass) position of each atom is not a quantum variable but described classically by the vector $\vec{r}_i(t) = \{0, 0, z_i^o + \upsilon t\}$. Obviously, such an assumption excludes several important effects on the atomic motion that arise due to quantization of the cavity field. For example, the correlations between the internal dynamics of the atoms and their transverse (center-of-mass) position may lead to an additional source of decoherence and disentanglement in the effective evolution (20), if the atom-cavity system is embedded in a realistic reservoir [19]. In our scheme, however, the external potential that is created by the optical lattice dominates the kinetic energy associated

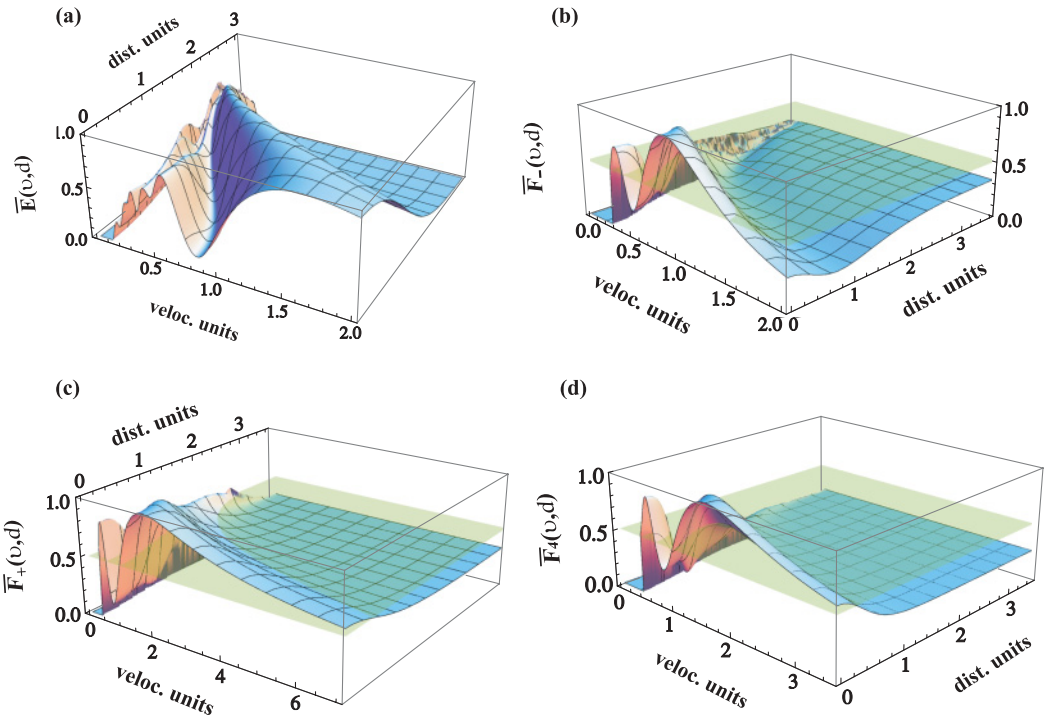

FIG. 7. (Color online) Entanglement and fidelity measures averaged over 20 randomly chosen uncertainties Δd and $\Delta \upsilon$ of the interatomic distance and the velocity, respectively. (a) Von Neuman entropy $\overline{E}(\upsilon, d)$, (b) fidelities $\overline{F}_{-}(\upsilon, d)$ and (c) $\overline{F}_{+}(\upsilon, d)$ for a chain of three atoms, and (d) $\overline{F}_4(\upsilon, d)$ for a chain of four atoms. The uncertainties for the distance and velocities are chosen from the intervals $[0, 0.2\,\overline{d}]$ and $[0, 0.1\,\overline{\upsilon}]$, respectively (see text for further details).

with the atomic momentum. Therefore, any correlations which are induced by the mechanical effects of cavity on atoms are strongly suppressed and have been neglected in our treatment.

V. SUMMARY AND OUTLOOK

A scheme is proposed to generate the entangled W states for a chain of N four-level atoms that are equally separated and conveyed through an optical cavity by means of an optical lattice. This scheme is based on the cavity-laser mediated interaction between the atoms which are separated by a macroscopic distance and works in a completely deterministic way for qubits encoded by two hyperfine levels of the atoms. Only two parameters, namely the velocity υ of the chain and the interatomic distance d, determine the effective interaction among the atoms and, thus, the degree of entanglement that is obtained for the overall chain. The asymptotic coupling (23) that completely characterizes the atomic evolution tells explicitly how the degree of entanglement depends on these two parameters. The purpose of this work is to understand the state evolution of the atomic chain and how it can be utilized to generate the entangled W states. For chains consisting of $N = 2, 3, 4$, and 5 atoms, Figs. 3–6 display the von Neumann entropy and the fidelities as functions of the velocity and interatomic distance. For $5 \leqslant N < 15$, moreover, we suggested the reference state (47) which is approximated by the wave function $|\Phi'_N\rangle$ with a high fidelity. In view of the recent developments in cavity QED, moreover, we have also analyzed and discussed the proposed scheme with regard to sensitivity in the formation of desired entanglement due to uncertainties in the atomic motion.

For two or more atoms, the generation of entanglement by means of a (detuned) optical cavity has been investigated in several articles [15,16,20]. All these studies, however, relied on the *small sample approximation* in which the separation of the atoms is considered to be negligible when compared with the cavity waist. Only recently [21–23], the atom-cavity coupling (5) has been exploited in more detail in order to suggest various entanglement schemes within cavity QED. In the work by Amniat-Talab *et al.*, for instance, a scheme was proposed in which two atoms were coupled sequentially to a resonant cavity and where a position-dependent coupling is used to drive a STIRAP-type process in order to reduce the losses due to atomic and cavity decays. Moreover, the scheme by Marr *et al.* is also based on a STIRAP-type process and describes an adiabatic evolution of a product state of two atoms which are coupled simultaneously to a detuned cavity. The success of this scheme, however, relies strongly on the ability to detect the photons which leak through the cavity mirrors with an efficiency close to one. In both schemes, therefore, the atomic velocities and interatomic separation are used to control the accuracy of a STIRAP-type process, in contrast to our approach, in which these parameters are utilized to control the degree of entanglement.

Our proposed scheme might be suitable also for ion-cavity experiments in which N trapped ions interact simultaneously with a (detuned) optical cavity [24,25]. In these experiments, the same coupling to the laser and cavity fields applies for ions with a three-level Λ-type configuration [as displayed

in Fig. 2(b)]. For such a level configuration, the qubit is associated with the states $|1\rangle$ and $|a\rangle$, and the W state can be generated by moving the equally distanced trapped ions along the trap. Similarly as for the atomic chains above, the cavity-laser-mediated interaction between the ions is described by the effective Hamiltonian (20) and, therefore, requires the same analysis as performed in Secs. III A– III D in order to produce the W_N states.

Finally, we like to mention our recent article [26] in which another deterministic scheme for generation of the multipartite W states has been proposed. In contrast to this work, the resonant atom-cavity interaction regime has been exploited for N flying two-level (Rydberg) atoms which couple sequentially (one after another) to the mode(s) of a high-finesse bimodal cavity.

ACKNOWLEDGMENTS

This work was supported by the DFG under the Project No. FR 1251/13.

[1] C. H. Bennett and S. J. Wiesner, Phys. Rev. Lett. **69**, 2881 (1992).
[2] A. K. Ekert, Phys. Rev. Lett. **67**, 661 (1991).
[3] L. K. Grover, Phys. Rev. Lett. **79**, 325 (1997).
[4] B. Weber, H. P. Specht, T. Muller, J. Bochmann, M. Mucke, D. L. Moehring, and G. Rempe, Phys. Rev. Lett. **102**, 030501 (2009).
[5] M. Khudaverdyan, W. Alt, T. Kampschulte, S. Reick, A. Thobe, A. Widera, and D. Meschede, Phys. Rev. Lett. **103**, 123006 (2009).
[6] M. P. A. Jones, J. Beugnon, A. Gaetan, J. Zhang, G. Messin, A. Browaeys, and P. Grangier, Phys. Rev. A **75**, 040301(R) (2007).
[7] D. Schrader, I. Dotsenko, M. Khudaverdyan, Y. Miroshnychenko, A. Rauschenbeutel, and D Meschede, Phys. Rev. Lett. **93**, 150501 (2004).
[8] D. D. Yavuz, P. B. Kulatunga, E. Urban, T. A. Johnson, N. Proite, T. Henage, T. G. Walker, and M. Saffman, Phys. Rev. Lett. **96**, 063001 (2006).
[9] S. Kuhr *et al.*, Science **293**, 278 (2001).
[10] S. Nussmann, M. Hijlkema, B. Weber, F. Rohde, G. Rempe, and A. Kuhn, Phys. Rev. Lett. **95**, 173602 (2005).
[11] K. M. Fortier, S. Y. Kim, M. J. Gibbons, P. Ahmadi, and M. S. Chapman, Phys. Rev. Lett. **98**, 233601 (2007).
[12] M. Khudaverdyan *et al.*, New J. Phys. **10**, 073023 (2008).
[13] D. Gonta and S. Fritzsche, J. Phys. B **42**, 145508 (2009).
[14] W. Dür, G. Vidal, and J. I. Cirac, Phys. Rev. A **62**, 062314 (2000).
[15] L. You, X. X. Yi, and X. H. Su, Phys. Rev. A **67**, 032308 (2003).
[16] S.-B. Zheng and G.-C. Guo, Phys. Rev. Lett. **85**, 2392 (2000).
[17] M. A. Nielsen and I. L. Chuang, *Quantum Computation and Quantum Information* (Cambridge University Press, Cambridge, 2000).
[18] H. Carmichael, *An Open System Approach to Quantum Optics* (Springer, Berlin, 1993).
[19] A. Varlica and G. Vetri, Eur. Phys. J. D **54**, 9 (2009).
[20] G.-P. Guo, C.-F. Li, J. Li, and G.-C. Guo, Phys. Rev. A **65**, 042102 (2002).
[21] M. Amniat-Talab, S. Guérin, N. Sangouard, and H. R. Jauslin, Phys. Rev. A **71**, 023805 (2005); M. Amniat-Talab, R. Nader Ali, S. Guérin, and M. Saadati Niari, Opt. Commun. **283**, 622 (2010).
[22] C. Marr, A. Beige, and G. Rempe, Phys. Rev. A **68**, 033817 (2003).
[23] Y. Li, C. Bruder, and C. P. Sun, Phys. Rev. A **75**, 032302 (2007).
[24] G. R. Guthöhrlein, M. Keller, K. Hayasaka, W. Lange, and H. Walther, Nature **414**, 49 (2001); M. Keller, B. Lange, K. Hayasaka, W. Lange, and H. Walther, *ibid.* **431**, 1075 (2004).
[25] A. B. Mundt, A. Kreuter, C. Becher, D. Leibfried, J. Eschner, F. Schmidt-Kaler, and R. Blatt, Phys. Rev. Lett. **89**, 103001 (2002); A. Kreuter, C. Becher, G. P. T. Lancaster, A. B. Mundt, C. Russo, H. Haffner, C. Roos, J. Eschner, F. Schmidt-Kaler, and R. Blatt, *ibid.* **92**, 203002 (2004).
[26] D. Gonta, S. Fritzsche, and T. Radtke, Phys. Rev. A **77**, 062312 (2008).